Technical Note: A novel leaf sequencing optimization algorithm which considers previous underdose and overdose events for MLC tracking radiotherapy

Eric Wisotzky,[a),b)] Ricky O'Brien, and Paul J. Keall[c)]
Radiation Physics Laboratory, Sydney Medical School, University of Sydney, Sydney, NSW 2006, Australia

(Received 31 August 2015; revised 15 October 2015; accepted for publication 16 November 2015; published 22 December 2015)

Purpose: Multileaf collimator (MLC) tracking radiotherapy is complex as the beam pattern needs to be modified due to the planned intensity modulation as well as the real-time target motion. The target motion cannot be planned; therefore, the modified beam pattern differs from the original plan and the MLC sequence needs to be recomputed online. Current MLC tracking algorithms use a greedy heuristic in that they optimize for a given time, but ignore past errors. To overcome this problem, the authors have developed and improved an algorithm that minimizes large underdose and overdose regions. Additionally, previous underdose and overdose events are taken into account to avoid regions with high quantity of dose events.
Methods: The authors improved the existing MLC motion control algorithm by introducing a cumulative underdose/overdose map. This map represents the actual projection of the planned tumor shape and logs occurring dose events at each specific regions. These events have an impact on the dose cost calculation and reduce recurrence of dose events at each region. The authors studied the improvement of the new temporal optimization algorithm in terms of the L1-norm minimization of the sum of overdose and underdose compared to not accounting for previous dose events. For evaluation, the authors simulated the delivery of 5 conformal and 14 intensity-modulated radiotherapy (IMRT)-plans with 7 3D patient measured tumor motion traces.
Results: Simulations with conformal shapes showed an improvement of L1-norm up to 8.5% after 100 MLC modification steps. Experiments showed comparable improvements with the same type of treatment plans.
Conclusions: A novel leaf sequencing optimization algorithm which considers previous dose events for MLC tracking radiotherapy has been developed and investigated. Reductions in underdose/overdose are observed for conformal and IMRT delivery. © *2016 American Association of Physicists in Medicine.* [http://dx.doi.org/10.1118/1.4937781]

Key words: multileaf collimator leaf sequencing, organ motion, adaptive reshaping, tumor motion control, cost optimization

1. INTRODUCTION

Radiation therapy aims to control the cell growth of tumor targets by delivering radiation dose to the target. To spare healthy tissue during treatment, high precision of the beam delivery and the beam shape is required, but anatomical motion during treatment causes misalignment between anatomy and beam shape. To reduce this intrafractional misalignment, tumor tracking has been introduced to synchronize the beam shape with the tumor motion.[1–6] This synchronization is done by modifying the position of the beam during treatment.

Intrafractional target motion in multileaf collimator (MLC) tracking radiotherapy requires the MLC to deliver online modified beam shapes. These shapes are different from the previous planned tumor shapes. After the target has moved during treatment and the new position is detected in real time, the MLC adapts the planned shape and delivers a modified beam shape. Managing complex motion pattern as well as complex beam shapes demands a systematic approach for MLC adaptation. Additionally, this shape adaption results in three different types of MLC aperture errors.[7] The first error, which due to the target position can only be estimated, is called localization error. Second, the leaf fitting errors are caused by the finite leaf width and finally, the leaf adjustment errors are due to the finite leaf speed. Full-fledged replanning in real-time would be the most ideal solution to overcome these problems. However, this is impractical due to heavy computation and on as-yet unresolved quality assurance issue.[8,9]

In this work, we expand the first order approximation to ideal online replanning introduced by Ruan and Keall.[10] In this first order optimization approach, the MLC leaf configuration is adapted by calculating the optimal leaf pair position according to the current tumor position. In this setup, undeliverable shapes occur, e.g., undeliverable shapes occur when the shape partially overlaps a leaf pair. In this case, the leaves can be fully closed, which underdoses the edge of the tumor, or fully open which overdoses healthy tissue. These undeliverable shapes result in overdose and underdose events, which we will refer to as dose events, caused by the aperture errors introduced above. Further events appear,

since the target is continuously moving while the framework calculates the new MLC setup and the leaves are adapting to the new positions. To minimize the MLC aperture errors and the resulting dose events, we use previous underdose and overdose information in our improved leaf sequencing optimization algorithm to calculate the optimal new shape. This technical note introduces a novel optimization framework expansion.

2. MATERIAL AND METHODS

We formulated the optimization problem in a constrained optimization algorithm with a dose map as input. In this dose map, all previous overdose and underdose events are recorded with their specific position. The optimization algorithm calculates the leaf sequence parameters that minimize the integrated overdose and underdose cost over all regions from the beginning of treatment till the actual time step, i.e., the optimization process is minimizing the L1-norm of the cumulative dose error. The optimal solution is derived by shifting the overdose/underdose map according to the detected intrafractional target displacement and including the previous occurred dose error in the optimization process. The separability of the cost across various leaf tracks allows us to improve the efficiency of the optimization algorithm and to consider each leaf track independently. We integrated the algorithm into an existing in-house developed framework.[11]

2.A. Mathematical optimization formulation

This section discusses the leaf sequencing optimization problem in the presence of motion. We assume a given tumor shape $f(x,y)$ and an estimated anatomical motion pattern $T(t)$, collapsed onto the beam's eye view (BEV). The ideal motion-compensated shape g is given by combining $f(x,y)$ with the collapsed BEV motion, resulting in the function $g = f \circ T$. The (x,y)-plane is located in the BEV, see Fig. 1.

The function $g(x,y,t)$, where (x,y) denotes the element location at a certain time point t, can be seen as a binary function over the region-of-interest (ROI): $\Omega \to \{0,1\}$, so that

$$g(x,y,t) = \begin{cases} 1 & (x,y,t) \in \text{transformed shape opening} \\ 0 & \text{else} \end{cases}.$$

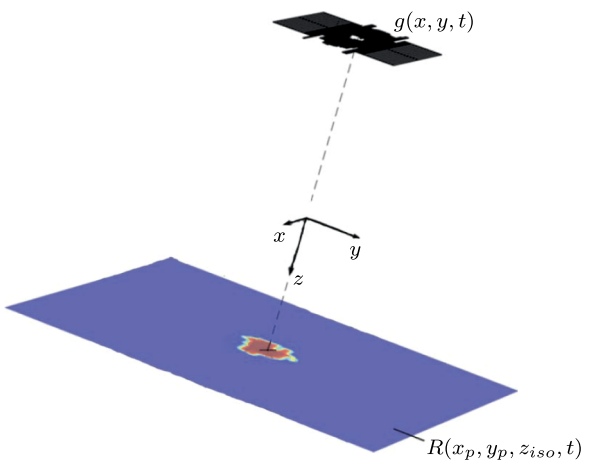

FIG. 1. This shows the basic setup. The MLC is located between treatment beam and target $R(x_p, y_p, z_{iso}, t)$.

Without loss of generality, we align the x-coordinate with the leaf track direction. Let Δ be the leaf resolution and located along y-direction. The complete aperture consists of N leaf pairs, starting at $y = 0$. With these specifications, the optimization problem can be described as finding the optimal position for every leaf pair, which fits the transformed tumor shape at a specific time point τ best and takes previous overdose and underdose events into account.

The leaf pair positions are parametrized as L_i for the left leaf position and R_i for the right leaf position, where the index $i = 1,2,\ldots,N$ describes the leaf pair. The optimization objective is quantitatively defined as the discrepancy between the deliverable shape parametrized by $\{L_i,R_i\}_{i=1}^{N}$ and the requested transformed tumor shape $g(x,y,t)$. Motivated by the therapeutic intent, this discrepancy is characterized as the sum of underdose and overdose costs, $\sum \lambda_u(x,y)$ and $\sum \lambda_o(x,y)$, respectively. For the tumor shape, the underdose cost $\lambda_u^{\text{tumor}}(x,y)$ is essential and initialized with 1, while the overdose $\lambda_o^{\text{tumor}}(x,y)$ is 0 and for the radio-sensitive healthy tissue, the overdose cost $\lambda_o^{\text{tissue}}(x,y)$ becomes important and is initialized with 1 while the underdose $\lambda_u^{\text{tissue}}(x,y)$ is set to 0. Underdose and overdose cost can be combined to a λ-map. These maps λ_o and λ_u contain the overdose and underdose events of every treatment step. Therefore, the optimization problem aims to find the L_i/R_i position for every leaf pair i, which minimizes the overall sum of overdose cost $\Phi_{i,o}$ and underdose cost $\Phi_{i,u}$ considering actual and previous overdose and underdose events,

$$\min \sum_i \sum_t (\Phi_{i,o}(t) + \Phi_{i,u}(t)).$$

To take previous overdose and underdose events into account, the cost maps λ_o and λ_u are time dependent and "collect" all occurring overdose and underdose events by increasing the weighting at this point (x,y) by 1. Assuming the leaves are of widths Δ, then the underdose cost and overdose cost for leaf track i are given at a certain point of time τ by

$$\Phi_{i,u}(\tau) = \int_{(i-1)\Delta}^{i\Delta} \int_0^{x_{\max}} \left(\int_0^{\tau} \lambda_u(x,y,t)dt \right) g(x,y,\tau) \times [I(L_i - x) + I(x - R_i)]dxdy$$

and

$$\Phi_{i,o}(\tau) = \int_{(i-1)\Delta}^{i\Delta} \int_0^{x_{\max}} \left(\int_0^{\tau} \lambda_o(x,y,t)dt \right) (1 - g(x,y,\tau)) \times [I(x - L_i)I(R_i - x)]dxdy,$$

while I is the indicator function and the following optimization needs to be solved:

$$\min \Phi_i(\tau) = \min(\Phi_{i,u}(\tau) + \Phi_{i,o}(\tau)).$$

For simplicity, we ignore in this mathematical description the leaf velocity. This condition can be included by introducing additional constraints on the optimization process.

Due to the fact that only λ and g are dependent on y and both are independent of L_i and R_i, we can reduce the cost functions to one dimension,

$$\Phi_{i,u}(\tau) = \int_0^{x_{\max}} c_{i,u}(x,\tau)[I(L_i - x) + I(x - R_i)]dx$$

and

$$\Phi_{i,o}(\tau) = \int_0^{x_{\max}} c_{i,o}(x,\tau)[I(x - L_i)I(R_i - x)]dx,$$

where the function $c(x,\tau)$ includes

$$c_{i,u}(x,\tau) = \int_{(i-1)\Delta}^{i\Delta} \left(\int_0^{\tau} \lambda_u(x,y,t)dt \right) g(x,y,\tau)dy$$

as well as

$$c_{i,o}(x,\tau) = \int_{(i-1)\Delta}^{i\Delta} \left(\int_0^{\tau} \lambda_o(x,y,t)dt \right) (1 - g(x,y,\tau))dy.$$

The function $c(x,\tau)$ includes the information of the λ-map and can be understood as a weighting factor for a specific position x, while $\Phi(\tau)$ provides the optimal L_i- and R_i-leaf position.

2.B. Solving the optimization problem

We implemented this optimization process in our existing treatment framework and without any restriction, we can combine both λ-maps to an underdose/overdose map where the overdose areas of the radio-sensitive tissue are initialized with $+1$, while the underdose areas of the tumor shape are initialized with -1, see Fig. 2. Occurring underdose or overdose events increase the value in the map by -1 or $+1$, respectively, at the occurring position (x,y). To ensure that the global minimum of the problem is found, we expand the optimization formula with its variance.

Therefore, the optimization formula is split into three cases and formulated as

$$\min \Phi_i'(\tau) = \min\left(\Phi_{i,1}(\tau)^2 + \Phi_{i,2}(\tau)^2 + \Phi_{i,3}(\tau)^2\right),$$

with

$$\Phi_{i,1}(\tau) = \int_0^{L_i} c_{i,u}(x,\tau)dx,$$

$$\Phi_{i,2}(\tau) = \int_{L_i}^{R_i} c_{i,o}(x,\tau)dx,$$

and

$$\Phi_{i,3}(\tau) = \int_{R_i}^{x_{\max}} c_{i,u}(x,\tau)dx,$$

where $\Phi_{i,1}(\tau)$ and $\Phi_{i,3}(\tau)$ describe the underdose cost associated with the region covered by the left and right leaf, respectively, and $\Phi_{i,2}(\tau)$ describes the overdose cost between the two leaves. The left and right leaf position are only related by the constraint that $L_i \le R_i$. Therefore, the first order condition for optimality is

$$\frac{\partial}{\partial(L_i)}\Phi_i'|_{L_i=x} = 0, \qquad \frac{\partial}{\partial(R_i)}\Phi_i'|_{R_i=x} = 0$$

and the second order condition becomes

$$\frac{\partial^2}{\partial(L_i)^2}\Phi_i'|_{L_i=x} > 0, \qquad \frac{\partial^2}{\partial(R_i)^2}\Phi_i'|_{R_i=x} > 0.$$

2.C. Experiments

To reduce the complexity of the problem, we started to implement our algorithm for 2D step and shoot intensity-modulated radiotherapy (IMRT), where we only needed a 2D-λ-map. We simulated the delivery of five conformal and fourteen IMRT-plans with seven 3D patient measured tumor motion traces. We simulated 100 MLC modification steps and evaluated the efficiency of our leaf sequencing optimization algorithm by calculating the mean absolute dose error (L1-norm), as well as the increase of the mean absolute error (MAE) at every step for the resulting 2D-λ-map. We used patient planned shapes for our simulations; therefore, the shapes were simple in their complexity, which means that the planned treatment shape is aligned to the MLC and in absence of tumor motion, the shape can be perfectly reproduced by the MLC. To increase the complexity of the shapes during simulation, we also rotated the shapes by 90° to obtain extreme shapes that cannot be perfectly reproduced by the MLC. This 90° rotation is not likely to occur clinically, but if we find an improvement for this extreme case, we make sure that in the whole interval from 0° to 90° rotations improvement can be reached. To confirm our simulated results, we performed IMRT experiments at a Varian Clinac machine. For these experiments, we used one 3D patient planned tumor shape and two 3D patient measured tumor motion traces; one trace is shown in Fig. 3. The delivered dose information were

FIG. 2. This is an example of an initialized underdose/overdose map. The planned tumor shape is white, while the shape that is not meant to be treated is black.

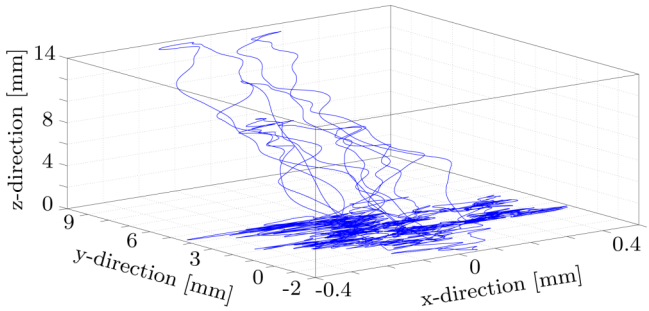

FIG. 3. This is a patients measured motion trace we used for our experiments at the Varian Clinac machine.

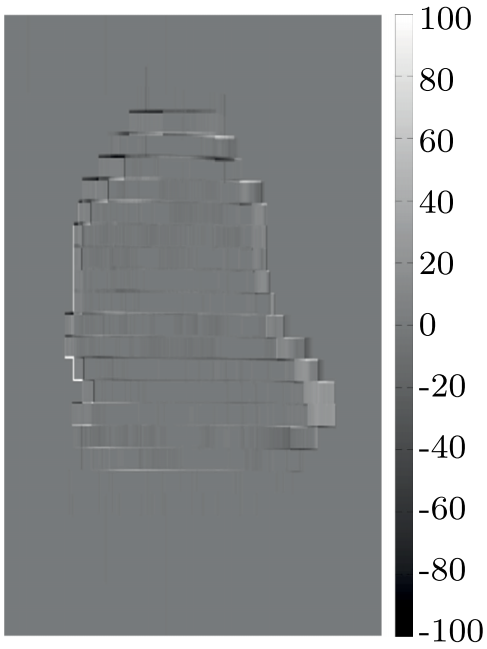

FIG. 4. This overdose/underdose map shows results after 100 steps for the IMRT experiments. In the large gray areas no dose events have occurred, while in the lighter areas overdose and in the darker areas underdose events happened.

measured by our framework; we logged the actual and needed leave positions and delivered dose and the λ-map (Fig. 4). Using this information, we were able to evaluate the improvement of our optimization algorithm without the need for a phantom. The time interval of motion tracking is 40 ms; therefore, our optimized leaf positions need to be calculated in this time period.

3. RESULTS

Simulations of conformal shapes showed an improvement of L1-norm up to 8.5% after 100 MLC modification steps. The improvement in terms of L1-norm for a single step increased by up to 18.2%. For every simulated case, an improvement of MAE can be achieved. As it can be seen in Table I, the improvement of MAE varies between simulation setups. For shapes that are aligned to the MLC, the improvement of our algorithm is about $1.45\% \pm 0.1\%$, because our algorithm improvements apply only for the case when the shape is exactly shifted by half of the leaf width. For more complex shapes, the improvement gets much larger, as for every single optimization step previous dose events affect the optimization result.

TABLE I. This table shows simulation results for two different kind of shapes with five different displacement amplitudes. All simulations are performed with the greedy heuristic algorithm by Ref. 10 and with our new temporally optimized algorithm. The mean absolute error (MAE) is calculated after 100 optimizations and the MAE increase displays the average L1-norm increase per step.

No.	Amplitude (mm)	Rotation (deg)	MAE greedy heuristic	MAE temporal optimized	MAE step increase greedy	MAE step increase optimized
1	35	0	1.79	1.77	0.0067	0.0065
2	30	0	1.70	1.68	0.0069	0.0066
3	25	0	1.71	1.68	0.0065	0.0063
4	15	0	1.71	1.69	0.0064	0.0062
5	15	90	1.84	1.77	0.0079	0.0072
6	00	90	1.97	1.80	0.0092	0.0075

TABLE II. This table shows experiment results of IMRT treatment with a maximum displacement of 16.9 mm. All experiments are performed with the greedy heuristic algorithm by Ref. 10 and with our new temporally optimized algorithm. No. 1 used a prostate treatment plan, while the others used a lung tumor plan.

No.	Amplitude average (mm)	MAE greedy heuristic	MAE temporal optimized	MAE step increase greedy	MAE step increase optimized
1	2.53	0.287	0.283	0.0031	0.0028
2	2.53	0.342	0.318	0.0040	0.0032
3	2.53	0.247	0.214	0.0025	0.0021

Experiments on a Varian Clinac machine confirmed our simulated results, see Table II. Numeral experiments with IMRT showed an improvement of up to 1.4% after the first 100 steps for prostate and up to 7.0% for lung treatments. For a single step, the average MAE improvement was $3.28\% \pm 0.4\%$ of all prostate treatment experiments. This improvement corresponds with our simulations and our expected improvement for simple shapes.

The runtime of our algorithm was on average 23.74 ms, but some cases were over 120 ms. The larger runtime can be reduced by running the optimization for separate leaves in parallel. The overall latency of tumor tracking systems is of the order of 200–300 and 23.74 ms is comparable to existing systems.[2–7]

4. CONCLUSION

A novel leaf sequencing optimization algorithm which considers previous dose events for MLC tracking radiotherapy has been developed and investigated. Reductions in underdose and overdose are observed for conformal and IMRT delivery. Our algorithm shows only a modest improvement when rotation is ignored, with a more significant improvement when rotation is included. Further improvements are expected as we transition to tracking general shapes, such as the fluence map produced during treatment planning. In this work, we have assumed that the treatment plan and fluence map remain invariant to patient motion. Online treatment replanning that takes into account leaf velocities, previous underdose/overdose, and the predicted tumor motion is the next logical step in tumor tracking software. Online replanning remains a challenge because of computation time and potential issues with QA and RT acceptance. The next step to improve our algorithm will be to extend and test it for volumetric intensity modulated arc therapy. Here, a 3D-λ-map is needed, where for every treatment angle, the corresponding

2D-λ-map is calculated using forward and backward projections. A 3D leaf sequencing optimization algorithm which considers previous underdose and overdose events could allow to use the planning target volume (PTV) or the clinical target volume (CTV) with internal margin as input for function $f(x,y)$. This would potentially further reduce the dose errors while increasing the treatment accuracy and is the first step to online treatment planning. In the future, we plan to improve our MLC motion control algorithm in terms of L1-norm dose error minimization by using more realistic and conformal shapes in the optimization process. We also plan to increase the robustness of the algorithm by optimizing the algorithm latency. Additionally, it is possible to include a L2-norm minimization into the algorithm to reduce overdose and underdose peaks in the patient.

ACKNOWLEDGMENTS

The authors would like to acknowledge the support of a National Health and Medical Research Council (NHMRC) Australia Fellowship.

[a]Electronic addresses: eric.wisotzky@charite.de and eric.wisotzky@ipk.fraunhofer.de
[b]Present address: Navigation, Robotics and Medical Technology, Charité Berlin, Augustenburger Platz 1, Berlin 13353, Germany. Also affiliated with Fraunhofer Institute for Production Systems and Design Technology (IPK), Pascalstr. 8-9, Berlin 10587, Germany.
[c]Electronic mail: paul.keall@sydney.edu.au

[1]P. J. Keall, V. R. Kini, S. S. Vedam, and R. Mohan, "Motion adaptive x-ray therapy: A feasibility study," Phys. Med. Biol. **46**, 1–10 (2001).
[2]A. Sawant, R. Venkat, V. Srivastava, D. Carlson, S. Povzner, H. Cattell, and P. J. Keall, "Management of three-dimensional intrafraction motion through real-time DMLC tracking," Med. Phys. **35**, 2050–2061 (2008).
[3]M. B. Tacke, S. Nill, A. Krauss, and U. Oelfke, "Real-time tumor tracking: Automatic compensation of target motion using the Siemens 160 MLC," Med. Phys. **37**, 753–761 (2010).
[4]S. P. M. Crijns, B. W. Raaymakers, and J. J. W. Lagendijk, "Proof of concept of MRI-guided tracked radiation delivery: Tracking one-dimensional motion," Phys. Med. Biol. **57**, 7863–7872 (2012).
[5]M. F. Fast, S. Nill, J. L. Bedford, and U. Oelfke, "Dynamic tumor tracking using the Elekta Agility MLC," Med. Phys. **41**, 111719 (5pp.) (2014).
[6]E. Wisotzky, M. F. Fast, U. Oelfke, and S. Nill, "Automated marker tracking using noisy x-ray images degraded by the treatment beam," Z. Med. Phys. **25**, 123–134 (2015).
[7]P. R. Poulsen, W. Fledelius, B. Cho, and P. J. Keall, "Image-based dynamic multileaf collimator tracking of moving targets during intensity-modulated arc therapy," Int. J. Radiat. Oncol., Biol., Phys. **83**, e265–e271 (2012).
[8]C. Wu, R. Jeraj, W. Lu, and T. R. Mackie, "Fast treatment plan modification with an over-relaxed Cimmino algorithm," Med. Phys. **31**, 191–200 (2004).
[9]R. Mohan, X. Zhang, H. Wang, Y. Kang, X. Wang, H. Liu, K. K. Ang, D. Kuban, and L. Dong, "Use of deformed intensity distributions for on-line modification of image-guided IMRT to account for interfractional anatomic changes," Int. J. Radiat. Oncol., Biol., Phys. **61**, 1258–1266 (2005).
[10]D. Ruan and P. J. Keall, "Dynamic multileaf collimator control for motion adaptive radiotherapy: An optimization approach," in *IEEE Power Engineering and Automation Conference* (IEEE, New York, NY, 2011), Vol. 3, pp. 100–103.
[11]P. J. Keall, E. Colvill, R. T. O'Brien, J. A. Ng, P. R. Poulsen, T. Eade, A. Kneebone, and J. T. Booth, "The first clinical implementation of electromagnetic transponder-guided MLC tracking," Med. Phys. **41**, 020702 (5pp.) (2014).